International Journal of Electrical and Computer Engineering (IJECE)
Vol. 9, No. 5, October 2019, pp. 3739~3750
ISSN: 2088-8708, DOI: 10.11591/ijece.v9i5.pp3739-3750

System integration of a fluoroscopic image calibration using robot assisted surgical guidance for distal locking process in closed intramedullary nailing of femur

Sakol Nakdhamabhorn, Jackrit Suthakorn
Department of Biomedical Engineering, Faculty of Engineering, Mahidol University, Thailand

Article Info

Article history:

Received Dec 12, 2018
Revised Apr 4, 2019
Accepted Apr 11, 2019

Keywords:

Fluoroscopic image calibration
close intramedullary nailing
Robot assisted surgical guidance
Surgical navigation system
Optical tracking device

ABSTRACT

Distal locking procedure is one of the most complex tasks in close intramedullary nailing operation which requires fluoroscopic image to interpret 2-D distal locking position on image related to 3-D distal locking position on the patient site. Hence the surgeon has to perform the distal locking process by using multiple fluoroscopic images which causes a lot of x-ray exposure to the patient and surgeon and is a time consuming task. This paper presents the system integration of a fluoroscopic image calibration using robot assisted surgical guidance. The system integration consists of three parts; distal locking recovery, fluoroscopic calibration and tracking, and robot assisted surgical guidance. The distal locking-hole recovery algorithm is based on characteristic information of the major and minor axes of distal locking hole. The fluoroscopic calibration and tracking is modeled as pin-hole projection model to estimate a projection equation based on optical tracking system. The robot-assisted surgical guidance is developed to overlay a trajectory path using a laser beam for reducing the problem of hand – eye coordination on most surgical navigation system. We integrate each part to complete a surgical navigation system for distal locking process.
The experiment of system integration is conducted to validate the accuracy of distal locking axis position and orientation. The results of the system integration shows a mean angular error of 1.10 and mean Euclidean distance in X-Y plane error of 3.65 mm.

Corresponding Author:

Jackrit Suthakorn,
Department of Biomedical Engineering,
Faculty of Engineering, Mahidol University, Thailand.
Email: jackrit.sut@mahidol.ac.th jackrit@bartlab.org

1. INTRODUCTION

Engineering and healthcare are and have been an important part of human life. Recently, engineering has paid more attention to and has had an influence on several healthcare procedures [1, 2]. Computer-Integrated Surgery (CIS) and Robot-Assisted Surgery (RAS) [3] play important roles in numerous medical operations and procedures. An important section of CIS/RAS is “medical navigation” which involves surgical planning and guiding in pre- and intra-operative procedures. Orthopedic surgery is one of the most common operations conducted in hospitals. In which one of the most common injury cases are of long bone fractures. There are many cases of orthopedic surgeries that are conducted in the hospitals on a daily basis. Orthopedic surgeries require much more accuracy in the procedure than the actual time taken in the surgical process itself. Therefore, these surgeries require highly experienced surgeons to perform these tasks. However, the scarcity of experienced surgeons available at any given may not be enough as the number of the patients waiting for treatments. Closed intramedullary nailing is a frequent procedure and efficient technique to treat long bone fractures. This technique requires the surgeon to insert an intramedullary nail into the bone canal of the fractured long bone, such as, femur, tibia and humorous, after bone-fixing process. The intramedullary nail is used as an internal structure to hold the fractures together in their proper shapes.

Figure 1 shows the intramedullary nail after inserted into the fractured bone. Closed Nailing is a minimally invasive surgery (MIS) which requires only a few small incisions during the process. However, medical image-guiding techniques are required. Fluoroscopic system (C-arm) is frequently used in this process. At the end of Closed Nailing process, the surgeon is required to perform nail locking process which includes proximal locking process as shown in Figure 1 (a) and distal locking processes as shown in Figure 1 (b). These locking processes are to insert two screws into the proximal locking and distal locking holes on the nail to keep the fractures in place. However, during the nail insertion process, the nail might get deformed and bent, which can be caused by external forces and torques [4]. The difficulty is to identify the position and orientation of the distal holes' axis, and to guide the surgeons to perform their tasks properly. In conventional method, surgeon uses fluoroscopic images to locate and identify the position and orientation of a distal locking hole of intramedullary nail. The surgeon uses trial and error method to align the fluoroscopic system into the right direction until the distal locking hole appears in a perfect circular shape on the display. Therefore, the axis of imaging components on fluoroscopic system is the same as the distal holes' axis, which helps/assists the surgeon to use as a guiding part for screw inserting in distal locking process. Thus, surgeon needs to realize a three-dimensional screw inserting based on two-dimensional fluoroscopic image. Therefore, large number of fluoroscopic images can be required for targeting the screw drilling trajectory. These require a lot of surgical time and produce a lot of x-ray radiation exposures during the operation which cause harmful effect of X-ray radiation exposure to both, the surgeon and the patient in their long term health and well-being. The overall radiation exposure time in this particular process can vary from 3 - 30 minutes and can take up to a few hours based upon the surgeon's skill and experience [5].

(a) (b)

Figure 1. The nail locking process in intramedullary of femur (a) The proximal locking (b) The distal locking

Several techniques and systems have been developed to overcome these difficulties. For example, a nail mounted targeting device, image intensifier mounted targeting device, self-locking nailing system, stereo - fluoroscopy and computer navigation system [6, 7]. However, these devices and techniques have several disadvantages, for example the lack of versatility of these devices, and practical user-interface. They are also not easy to use. Many Computer Integrated Surgery Systems have been proposed to assisted operations, especially in distal interlocking holes targeting. The approach for recover a position and orientation of distal-hole axis uses only the area of projected image to recover the nails rotation angle with respect to fitting curve technique [8, 9]. Thierry Leloup et. al, [10, 11] developed a technique of recovery of a distal locking hole which used only two fluoroscopic images with no need to capture the axis of the hole. A fluoroscopy is calibrated in pre-operation process using two parallel plates. The lower plate containing metallic balls element is used to calibrate image distortion and the upper plate containing metallic rings is used to determine the X-ray source position. The extrinsic of the upper calibration plate is attached with an optical tracking marker then metallic balls and metallic rings in both calibration plates can determine the locations relative to this optical marker.

Guoyan Zheng et al, [12, 13] developed an automatic recovery of distal interlocking hole. This work was based on a single calibrated and registered fluoroscopic image. They defined the recovery problem into a sequential two-stage model-base optimal fitting process. The fluoroscopic images were calibrated by using weak-perspective pin-hole camera model combined with optical tracking to relate a 2D pixel into 3D point and also correct a c-arm distortion. Yaniv and Joskowicz [14, 15] developed a precise robot assisted guide positioning for the distal locking intramedullary nail. This robot was a bone-mounted miniature robot fitted with a drill guide. The robot rigidly attached to the nail or the bone. Therefore, the system does not have any serious effect on the immobilization of the leg. The calibration method, they modeled the fluoroscopic as a pin-hole camera and calibrate fluoroscopic image distortion. Another system called “HIT-RAOS”, a system developed by Du Zhi-jiang [16], assists the surgeons thru many process during the close intramedullary nailing. Such as, to reposition broken bones, to guide the surgeon locking nail, to reduce the surgeon’s working under fluoroscopic system by tele-operation system. The augmented reality navigation system was developed to assisted surgeons during distal interlocking. The augmented radiolucent drill combined multi-modal visualization to track and overlay a drilling trajectory under a video-guided in real-time [17, 18]. The concept of surgical navigation for close intramedullary nailing of femur using an overlay laser guiding was proposed by Nakdhamabhorn and J.T. Liang [19, 20].

A system integration of Fluoroscopic image navigation system based Robot-Assisted Surgical Guidance system for distal locking process in Closed Intramedullary Nailing of Femur is proposed in this paper. The proposed approach is to integrate a system, which is able to generate a navigation trajectory path of distal locking holes drilling axis, and a robotic guidance system to interface with the surgeon to perform the tasks. The system consists of 4 major parts: (a) The recovery distal locking-hole axis with fluoroscopic images; (b) Fluoroscopic image calibration; (c) Fluoroscopic tracking for matching a spatial image coordinate (two-dimensional) into world reference coordinate (three-dimensional) using optical tracking system; (d) A novel Robot assisted surgical guidance by using a laser for navigating a drilling trajectory path.

2. RESEARCH METHOD

This paper presents a novel approach of integrating fluoroscopic image calibration and tracking system with Robot-Assisted Surgical Guidance system for distal locking process in Closed Intramedullary Nailing of Femur. The algorithms consist of Distal locking hole’s position and orientation recovery algorithm, the fluoroscopic image calibration, the fluoroscopic tracking, and the robot-assisting surgical guidance. These are described as subsection below.

2.1. System overview

The overview of the system is shown in Figure 2. The system is separated into pre-operative and intra-operative. In pre-operative, the fluoroscopic image calibration and the distal locking-hole recovery algorithm are performed to generate a set of calibration parameters which are required to implement in intra- operative. The fluoroscopic tracking involves in the intra-operative to transform two-dimensional position and orientation of distal locking hole to three-dimensional world coordinate by using calibrated parameters. At that point, the three-dimensional distal locking hole trajectory sends to Robot-Assisted guidance for generating a surgical guiding path.

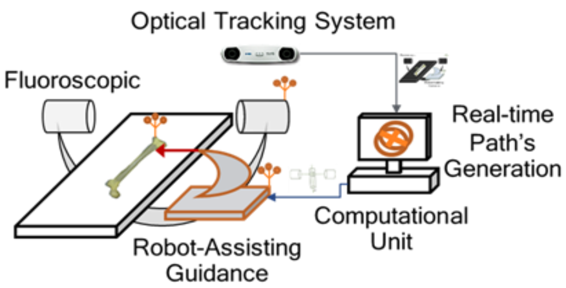

Figure 2. The overview of the system integration

2.2. Distal locking hole’s axis recovery

The distal locking hole’s recovery algorithm is applied to identify a position and orientation of distal locking hole’s axis based on a fluoroscopic image. To simplify a reference coordinate, the intramedullary nail is defined as a reference coordinate as shown in Figure 3(a). The X axis places along with the nail axis. The Z axis places along with distal locking-hole’s axis. In the operation, the translation and rotation are occurred only in X and Y direction.

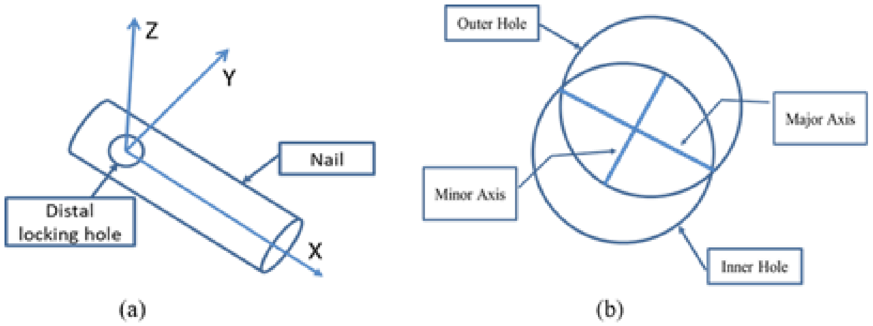

Figure 3. (a) A reference coordinate of an intramedullary nail
(b) The characteristics of the projection image of distal locking hole

The conventional method of locating the distal locking hole was completely reliant on the skills of a particular surgeon. The surgeon adjusts the angle of the fluoroscopic system to make a projection of distal locking hole image which appears as a circular shape. This algorithm uses only two fluoroscopic images to realize the distal locking-hole's axis. The algorithm utilizes characteristic information of the intramedullary nail, such as, nail radius, major and minor axes of distal locking hole, and the area of distal locking hole as shown in Figure 3(b).

The algorithm is separated into two iterations. The first iteration is the simulation process. In this process, the intramedullary nail is rotated in all possible projections. The visible projection of image appears at 0 to 30 degree of rotation. Then, the image is captured at 0, 2, 4, 6, 8, 10…, and 30 degrees of rotation to create simulated images. All the simulated nail images are then extracted in a ratio between the major and minor axes of the distal locking hole by using fitting ellipse image processing algorithm [21]. So, the ratio between the major and minor axis in each rotation angle, which is stored together with the *X-Y-Z* Euler rotational angle in a database. This part is done in the pre–operative process. The second iteration is for extracting information from the real-time distal locking-hole images. The edge detection and fitting ellipse techniques are applied to find a position and the characteristic of distal locking hole on an image. The ratio between major and minor axis of distal locking hole is then calculated in real-time matching process to recover a distal locking-hole's axis rotation. The cubic curve fitting is then applied to find the best fit to the data in the database. The tool curve is used to reversely recover the rotational angle of distal locking-hole's axis. This step is performed during the intra-operative process.

2.3. Fluoroscopic image calibration

The purpose of fluoroscopic image calibration is to determine the image distortion parameters and the image projection parameters. The fluoroscopic image calibration method requires a calibration phantom to create a set of calibration points which is used to calculate the image distortion parameters and the image projection parameters. The calibration phantom is made of squared acrylic material which is embedded with a dotted pattern of small metal balls as shown in Figure 4. The spatial distance within each dot pattern is 2 millimeters in both horizontal and vertical direction.

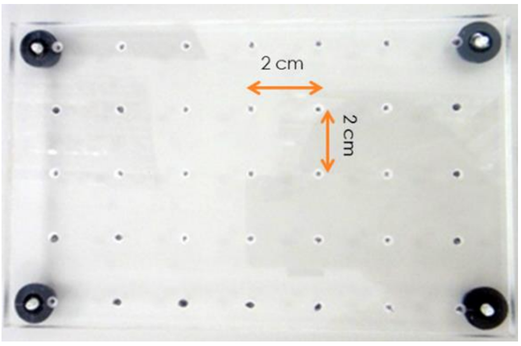

Figure 4. The calibration phantom

The fluoroscopic image has some distortion and the digital image from fluoroscopic system is distorted by the lens of fluoroscope and x-ray source. The distortion parameters are then added into the fluoroscopic image to re-correct the distorted image [22]. In section 2.2, the position and orientation of distal locking hole is based on the information of pixel image coordinate which is a two-dimensional image. Inappropriately, the drilling trajectory is represented in three-dimensional coordinate (world reference coordinate). Then, the fluoroscopic image calibration is applied to transform and track the relationship between two-dimensional image coordinate and three- dimensional world reference coordinate.

The objective of the projection calibration is to determine a projection matrix that transforms a three-dimensional point into a two-dimensional pixel point. The perspective projection (pinhole camera model) is defined as a geometric model. The model is based on projection characteristics which are the focal length, skewing parameter and center of the image projection. The projection parameters are constructed into the matrix called an “intrinsic matrix”. The transformation of image plane coordinate to world coordinate which is described in the transformation matrix called an “extrinsic matrix”. The pin-hole image projection is shown in (1).

$$\begin{bmatrix} x^{p} \\ y^{p} \\ 1 \end{bmatrix} = \begin{bmatrix} f_x & r & u_0 & 0 \\ 0 & f_y & v_0 & 0 \\ 0 & 0 & 1 & 0 \end{bmatrix} \begin{bmatrix} r_{11} & r_{12} & r_{13} & t_x \\ r_{21} & r_{22} & r_{23} & t_y \\ r_{31} & r_{32} & r_{33} & t_z \\ 0 & 0 & 0 & 1 \end{bmatrix} \begin{bmatrix} x^{w} \\ y^{w} \\ z^{w} \\ 1 \end{bmatrix} \tag{1}$$

Where f_x is a focal length on x axis, f_y is a focal length on y axis, which are scaled in millimeters respectively, r is a skewing parameter, u_0 and v_0 is the center of the image in pixel, r and t are translation and orientation of the image plane. The intrinsic matrix and extrinsic matrix in (1) are combined into a projection matrix P and rewritten as (2).

The projection matrix P is the transformation matrix, for transforming a world coordinate point (X, Y, Z) into a pixel coordinate point (u, v). The matrix P can be estimated by using the direct linear transformation (DLT) algorithm [23]. The extrinsic matrix is the position and orientation of the fluoroscopic image coordinate frame relative to the world coordinate. The intrinsic parameter consists of a focal length of the camera, scaling factors in the x and y direction and the center of the image plane in pixel.

$$\begin{bmatrix} X_1 & Y_1 & Z_1 & 1 & 0 & 0 & 0 & 0 & -u_1X_1 & -u_1Y_1 & -u_1Z_1 & -u_1 \\ 0 & 0 & 0 & 0 & X_1 & Y_1 & Z_1 & 1 & -v_1X_1 & -v_1Y_1 & -v_1Z_1 & -v_1 \\ X_2 & Y_2 & Z_2 & 1 & 0 & 0 & 0 & 0 & -u_2X_2 & -u_2Y_2 & -u_2Z_2 & -u_2 \\ 0 & 0 & 0 & 0 & X_2 & Y_2 & Z_2 & 1 & -v_2X_2 & -v_2Y_2 & -v_2Z_2 & -v_2 \\ & & & & & & \vdots \\ X_n & Y_n & Z_n & 1 & 0 & 0 & 0 & 0 & -u_nX_n & -u_nY_n & -u_nZ_n & -u_n \\ 0 & 0 & 0 & 0 & X_n & Y_n & Z_n & 1 & -v_nX_n & -v_nY_n & -v_nZ_n & -v_n \end{bmatrix} \begin{bmatrix} P_{11} \\ P_{12} \\ \vdots \\ P_{34} \end{bmatrix} = 0 \tag{2}$$

2.4. Fluoroscopic image registration and tracking

In this system, the optical tracking system is defined as a reference world coordinate. The system uses a commercial optical tracking “Polaris Vicra” from Northern Digital Inc. The optical Tracking system is a system for measurement of the position and orientation in a 3-dimensional active or passive marker. The active marker is made up of infrared light-emitting and the wireless passive marker is made up of a reflective sphere and therefore, the stereo camera receives light from the marker reflection or marker emission. The optical tracking system can identify and recognize the markers by the different pattern of markers shape. Then, the optical tracking system provides a three-dimensional position and orientation of the marker related to the optical tracking coordinate. The position is constructed in *3x1* position vector and the orientation is specified as *3x3* rotation matrix. The position vector is combined with rotation matrix to create the homogenous transformation matrix in (3) which is represented as a transformation between marker coordinate and the optical tracking reference coordinate.

$$H = \begin{bmatrix} R3x3 & T3x1 \\ 0\,0\,0 & 1 \end{bmatrix} \tag{3}$$

H is homogenous transformation; R is *3x3* rotation matrix; T is *3x1* positon vector.

Consequently, the homogenous transformation can be determined by attached markers to the object. In the system, the marker is attached with fluoroscopic system and Robot-assisted surgical guidance. The homogenous transformation relationship between each object can be determined with the homogenous transformation relationship [24] as illustrated in Figure 5.

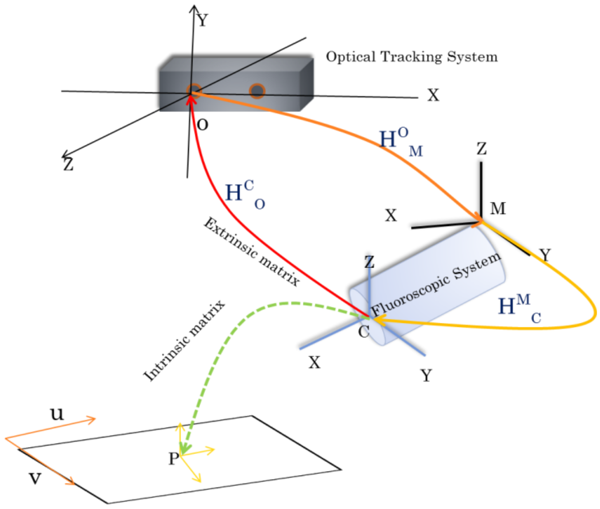

Figure 5. The homogenous transformation relationship of the calibration and tracking

The fluoroscopic image coordinate is defined as coordinate {C}. The homogenous transformation of image coordinate to optical tracking reference coordinate is ${}^{C}_{O}H$. The coordinate {M} represents the fluoroscopic system coordinate which ${}^{O}_{M}H$ is the homogenous transformation of optical tracking reference coordinate to fluoroscopic system coordinate. The ${}^{M}_{C}H$ is defined as the static homogenous transformation of coordinate {M} to coordinate {C} whenever, the fluoroscopic system moves, the static homogenous transformation ${}^{M}_{C}H$ will be constant.

Once the calibration process in section 2.1 is completed, the intrinsic and extrinsic matrix is calculated. The intrinsic parameter is a specific projection parameter of fluoroscopic image to project an object into an image plane. The extrinsic matrix is a homogenous transformation of the image coordinate related to the optical tracking coordinate which is equal to ${}^{C}_{O}H$. Then, the ${}^{M}_{C}H$ is calculated by (4).

$$ {}^{M}_{C}H = {}^{O}_{M}H^{-1}\,{}^{C}_{O}H^{-1} \quad (4) $$

In intra-operative, the fluoroscopic system is moved to capture a distal locking-hole image so the fluoroscopic image coordinate is changed as shown in Figure 6(b). In order to track the transformation of the fluoroscopic image coordinate {C}, the static homogenous transformation ${}^{M}_{C}H$ is used to calculate the new ${}^{C}_{O}H$ or new extrinsic matrix by (5)

$$ {}^{C}_{O}H = {}^{M}_{C}H^{-1}\;{}^{O}_{M}H^{-1} \quad (5) $$

Hence, the pin-hole image projection in (1) can be completed with a new extrinsic matrix. The tracking process updates a new extrinsic matrix to create a new projection equation. Therefore, the system can calculate a three-dimensional (X, Y, Z) position in reference coordinate by inputting the two-dimensional image pixel (u, v) coordinate. The equation of the relation between two-dimensional position and the three-dimensional position are shown in (6) and (7).

$$ u = f_x \frac{R_{11}X+R_{12}Y+R_{13}Z+t_1}{R_{31}X+R_{32}Y+R_{33}Z+t_3} + c_x \quad (6) $$

$$ v = f_y \frac{R_{21}X + R_{22}Y + R_{23}Z + t_2}{R_{31}X + R_{32}Y + R_{33}Z + t_3} + c_y \quad (7) $$

Where u, v are the input of the pixel position on the image, f_x is a focal length on x axis, f_y is a focal length on y axis, c_x and c_y is the center of the image in pixel, R and t are translation and orientation of the image plane.

2.5. Robot guidance system

In the surgical navigation system, our robotics guiding system is central to the process. This system interacts with the surgeon by using laser beam to overlay the distal locking drilling path. The guiding information of the several navigation systems are displayed via the monitor by demonstrating the animation graphics on the screen. Conversely, a surgeon would prefer during the operation, to pay more attention to the surgical site than on the screen. The proposed system eliminates the hand-eye coordination problem. The robot consists of four degrees of freedom, which are two translation joints and two rotation joints. The robot is attached at the Fluoroscopic system (C-Arm) as shown in Figure 6(a). After the navigation system generates the trajectory path, the robot is pointing a laser beam at the entry location while path orientation is also derived by comparing the drilling tool axis and the laser beam axis.

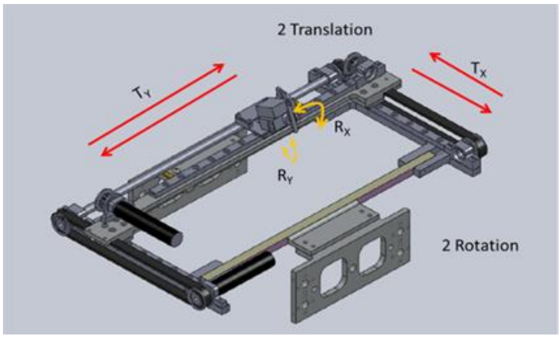

(a)

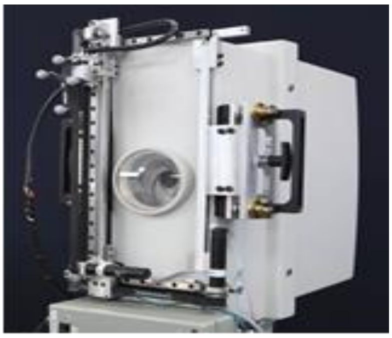

(b)

Figure 6. (a) CAD design model of the robot-assisted (b) The robot-assisted attaches with the C-Arm

The planar linear translation movement is generated by two translation joints, which is implemented by a linear guidance movement driven by a belt mechanism. The two rotation movements are used to adjust the orientation of laser beam aligned with distal locking axis. The end-effector of the robot is attached with a laser pointer in order to overlay the surgical drilling path. The robot is portable and can easily mounted on the fluoroscopic system. The low-level controller uses the PIC microcontroller with a position controller to control the DC motors and the servo motors [25].

3. RESULTS AND ANALYSIS

The following experiment is separated in two sections. Firstly, the distal locking-hole axis recovery algorithm which is implemented to recover the rotation of the drilling trajectory and the second experiment is integrated with the first experiment so as to complete the system integration of robot-assisted surgical guidance.

3.1. Experiment on distal locking hole’s axis rotation recovery

In the experiment, the algorithm of distal locking hole axis’s rotation recovery was implemented in a fluoroscopic system. The model of fluoroscopic system is a Philips BV Pulsera. The fluoroscopic images were captured via BNC port at the back panel of the fluoroscopic system. Then, the USB video frame grabber was used to capture the signal and then sent to the computer for processing. The testing image was captured at 5, 10, 15, 20 and 25 degrees of rotation of the intramedullary nail as shown in Figure 7. The image processing technique extracted information of those fluoroscopic images to make a dataset of “Tool curve” which is then stored in the database. This process was done during the pre-operative stage.

The fluoroscopic image was captured 10 times in each degree rotation during the intra-operation. The acquired image was extracted a feature of distal locking hole by image processing technique which then calculated the degree of rotation of C-arm by using curve fitting equation. The calculation process used a curve fitting equation. The result of C-arm degree of rotation was shown on the graphic user interface. The Figure 8 illustrates the image result, which shown on the graphic user interface of the program. The experiment was conducted fifty times with five different degrees of rotation (5^o, 10^o, 15^o, 20^o, and 25^o). The summary of the result is shown in Table 1. The average angular error is 1.15 degree of intramedullary nail rotation.

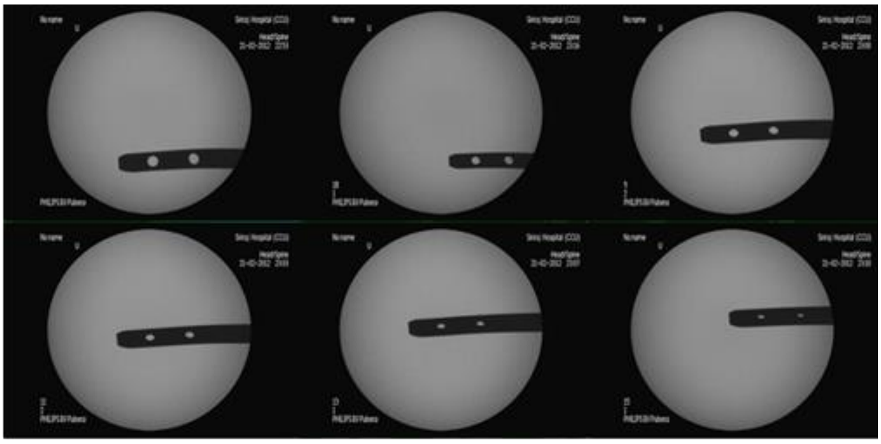

Figure 7. The distal locking hole images in each degree of rotation

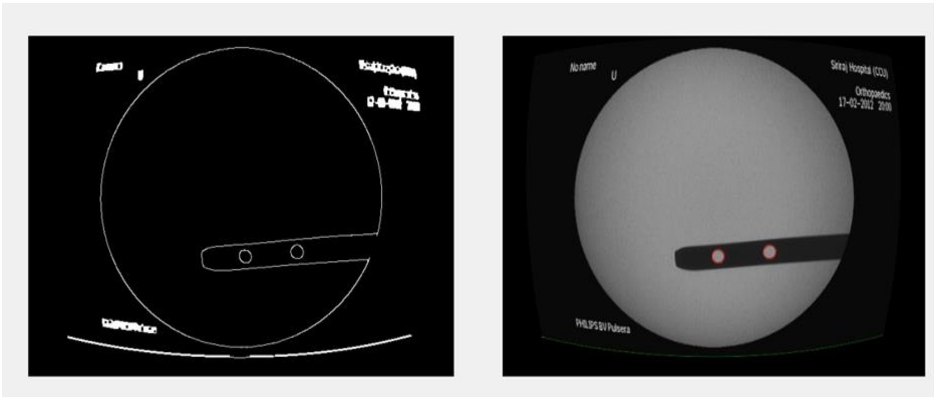

Figure 8. The Graphic user interface of the distal locking hole recovery program

Table 1. The summary of angular error of intramedullary nail rotation

Degree of intramedulary nail Rotation	The prediction angular error in degree of intrmedullary nail rotation			
	Max	Min	Average	SD
5	1.811	0.026	0.8426	0.7073
10	1.496	0.04	0.5819	0.4644
15	1.225	0.275	0.6406	0.4711
20	2.663	0.871	1.632	0.5988
25	3.945	0.086	2.0754	1.3688
total	3.945	0.026	1.1545	0.9708

3.2. Experiment on fluoroscopy calibration and system integration of robot-assisted guidance

The calibration method was separated into 2 operations during the experiment into pre-operative and intra-operative operation. The intra-operative experiment preforms 2 steps of fluoroscopic image calibration. The first step is fluoroscopic image distortion calibration and the second step is fluoroscopic image projection calibration. The experiment setup is shown in Figure 9. The optical tracking system is placed down behind the fluoroscopic system for setting up three-dimensional world reference coordinate. The optical marker and the robot-assisted surgical guidance system are attached to the fluoroscopic system.

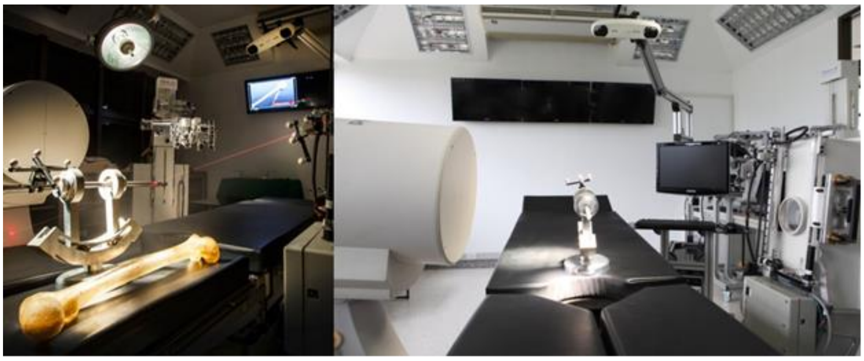

Figure 9. Integration of the robot-assisted surgical guidance system

3.2.1. Pre-operative

a. STEP I: Fluoroscopic image distortion calibration

The image distortion calibration was implemented to determine distortion co-efficient parameters. The distortion co-efficient parameters were used to correct the distortion of the fluoroscopic image. The set of calibration images were corrected in different position and orientation. The image processing technique was applied to segment a position of the calibration point in an image which corresponds with the spatial position of calibration points on the acrylic phantom. Twelve calibration phantom images were acquired to generate 300 corresponding calibration points. The corresponding calibration points were used to estimate the distortion parameters. The result of corrected image is shown in Figure 10.

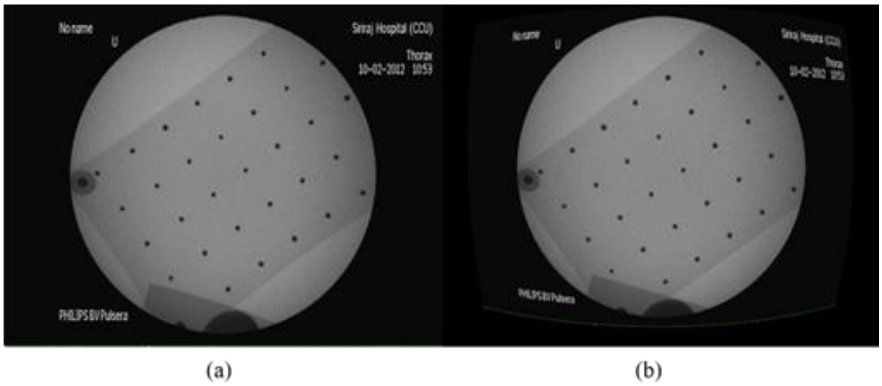

Figure 10. (a) Distorted calibration image (b) un-distorted calibration image

b. STEP II: Fluoroscopic image projection geometry calibration

The distortion parameter in step I was applied to correct the fluoroscopic calibration image, then the un-distortion image was segmented to the calibration point position on the image to create a set of two dimensional corresponding points. At the same time, the optical tracking system provided a three dimensional position of calibration point on the calibration phantom to generate a set of three dimensional corresponding points. The system acquired 12 calibration images to create 300 calibration points for estimating the projection matrix. The projection matrix was decomposed to intrinsic parameters and extrinsic parameters which described as projection (1). Then, the static homogeneous transformation (${}^{M}_{C}H$) can be determined by (4). The completed solution result of projection equation was shown in (8) and the result of (${}^{M}_{C}H$) homogeneous transformation was represented in (9).

$$\begin{bmatrix} u \\ v \\ 1 \end{bmatrix} = \begin{bmatrix} 1720 & 0 & 216.75 & 0 \\ 0 & 1556.7 & 958.15 & 0 \\ 0 & 0 & 1 & 0 \end{bmatrix} \begin{bmatrix} 0.292 & -0.774 & 0.561 & 695.366 \\ -0.640 & 0.277 & 0.7158 & 970.973 \\ -0.7099 & -0.568 & -0.415 & -734.348 \\ 0 & 0 & 0 & 1 \end{bmatrix} \begin{bmatrix} x^{w} \\ y^{w} \\ z^{w} \\ 1 \end{bmatrix} \quad (8)$$

$$ {}^{M}_{C}H = \begin{bmatrix} -0.021 & 0.428 & -0.903 & -274.522 \\ 0.993 & -0.092 & -0.067 & -33.893 \\ -0.112 & -0.898 & -0.423 & 109.1282 \\ 0 & 0 & 0 & 1 \end{bmatrix} \quad (9) $$

3.2.2. Intra-operative

After the calibration process in pre-operative stage was done, the distortion parameters, projection geometry parameters and the static homogenous transformation (${}^{M}_{C}H$) were implemented in intra-operation. The fluoroscopic system was moved to capture a distal locking hole image then the distortion parameters was used to correct the distortion of an image. The distal locking-hole recovery algorithm recovered an orientation of distal locking hole' axis then extracted distal locking-hole position on an image. The tracking system provided a real-time homogenous transformation of fluoroscopic system to calculate a new extrinsic matrix for constructing a projection equation then the precise three-dimensional position and orientation of distal locking hole was calculated by solving the projection equation. The robot-assisted surgical guidance received a three-dimensional position an orientation to generate a drilling trajectory path for guiding a surgeon as shown in Figure 9.

The system was tested with 5 different intramedullary nail rotations (5, 10, 15, 20 and 25 degree). The experiments were conducted with the 5 different degrees of rotation ten times each respectively, making a total of fifty experiments that were conducted. The translation error in each axis is shown in Figures 11-13. The spatial distance error in *X-Y* plane is summarized in Table 2.

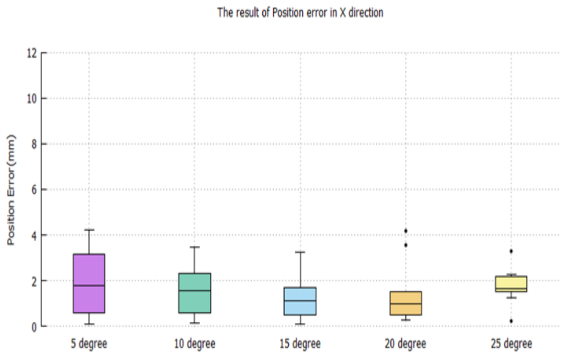

Figure 11. The result of position error in X direction

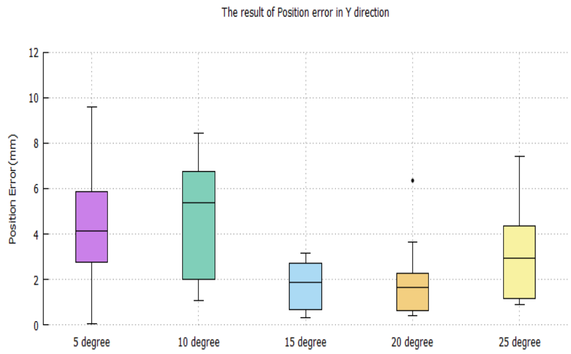

Figure 12. The result of position error in Y direction

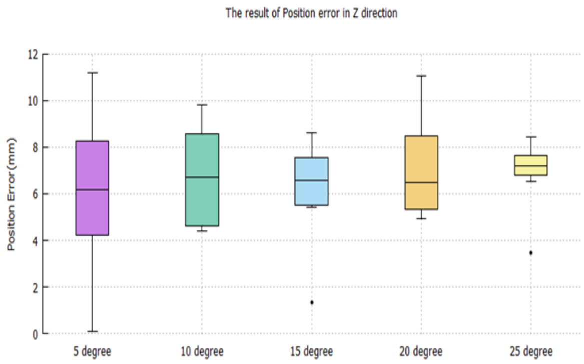

Figure 13. The result of position error in Z direction

Table 2. The summary of spatial distance error in x-y plane.

	Spatial distance error in X-Y plane (mm)		
	X	Y	Euclidean Distance(mm)
Min	0.073	0.052	0.090
Max	4.211	9.593	10.47
Mean	1.607	3.280	3.652

4. CONCLUSION

This paper proposes a new approach to the fluoroscopic navigation system using robot assisted surgical guidance for screw locking process in closed intramedullary nailing of femur. The system consists of four main parts, distal locking-hole recovery algorithm, fluoroscopic image calibration, fluoroscopic tracking, and robot-assisted surgical guidance. The image processing techniques are implemented based on the canny edge detection and fitting ellipse algorithm for extraction of the distal locking-hole position and the information of the major and minor axis. The curve fitting is used with the higher degree of the polynomial to predict the distal locking-hole rotation. The results of the algorithm as discussed in detail in the section 3 of this paper. The five rotation degrees of distal locking- hole rotation are tested with 5, 10, 15, 20, 25 degrees of rotation. The results of the experiments conducted show only a small error in rotation. The fluoroscopic image calibration algorithm based on the calibration phantom and the pinhole project equation which is applied to find the intrinsic and the extrinsic parameters. The fluoroscopic image calibration also calculates the distortion parameter to re-correct the distortion of the fluoroscopic image. The Fluoroscopic image calibration algorithm can be implemented on any fluoroscopy surgery application.

The robot assisted surgical guidance system is developed to guide the trajectory of the distal locking-hole axis. The robot is specifically designed so as to be able to attach with the Fluoroscopic system. The robot is designed as a portable robot, and can be plugged-in and out from the fluoroscopic system easily. The main purpose of robot assisted surgical guidance is to reduce the hand – eye coordination problem that is caused by using screen to display the surgical path. In conclusion, the four main parts are integrated into a complete surgical navigation system for distal locking process in closed intramedullary nailing of femur.

ACKNOWLEDGEMENTS

This research has been funded by the University-Industry Research collaboration (U-IRC) scholarship from The National Science and Technology Development Agency (NSTDA), Thailand for the financial support and also Government Research Budget through Mahidol University (Grant No. 111-2558). We would like to thank Siriraj Hospital surgeons and staffs for their valuable knowledge and recommendations towards the development of this system. Another group we would like to thank are the BARTLAB members who presented us with knowledge in mechanical design, programming and statistical analysis.

REFERENCES

[1] Sushma, S.J., Prasanna Kumar, S.C. “Advancement in research techniques on medical imaging processing for breast cancer detection,” *International Journal of Electrical and Computer Engineering (IJECE).*, vol. 6, no. 2, pp. 717-724, 2016.
[2] Hamiane, M., Saeed, F., “SVM classification of MRI brain images for computer-assisted diagnosis,” *International Journal of Electrical and Computer Engineering.*, vol. 7, pp. 2555-2564, 2017.
[3] Russell H. Taylor, D. Stoianovici, "Medical Robotics in Computer-Integrated Surgery," *IEEE Trans. Robot. Automat.,* vol. 19, pp. 765-781, 2003.
[4] J. M. C. Krettek, T. Miclau, P. Schandelmaier, I. Linnemann, and H. Tscherne, "Deformation of fermoral nails with intramedullary insertion," *J. Orthopaedic Res.,* vol. 16, pp. 572-575, 1998.
[5] S. Skjeldal and S. Backe "Interlocking medullary nails radiation doses in distal targeting," *Arch. Orthopaedic Trauma Surg,* vol. 106, pp. 179-181, 1987.
[6] G.M. Whatling, L. D. M. Nokes "Literature review of current techniques for the insertion of distel screws into intramedullary nails," *J. Care Injured,* vol. 37, pp. 109-119, 2006.
[7] R. Hofstetter, M. SlomczyKowski, L.-P. Nolte, “Fluoroscopy as an Imaging Means for Computer-Assisted Surgical Navigation,” *Computer Aided Surgery.*, vol. 4(2), pp.65-76, 1999.
[8] Neatpisarnvanit, C., and Suthakorn, J., "Intramedullary Nail Distal Hole Axis Estimation using Blob Analysis and Hough Transform," *Proceedings of the 2006 IEEE International Conference on Robotics, Automation and Manufacturing*, pp. 1-6, 2006.
[9] Nakdhamabhorn, S., and Suthakorn, J., "On the Design and Experiments of a Fluoro-Robotic Navigation System for Closed Intramedullary Nailing of Femur," Recent Advances in Computer Science and Information Engineering Vol 2: *Springer Tracts in Lecture Notes in Electrical Engineering*, Vol. 125, Qian, Z.; Cao, L.; and Su, W. (Eds),Publisher, Springer-Verlag Berlin Heidelberg, ISBN: 978-3-642-25789-6 pp 195-202, 2012.
[10] T. Leloup, W. E. Kazzi, O. Debeir, F. Schuind, and N. Waree, "Automatic flouroscopic image calibration for Traumatology Intervention Guidance," *Proc. Int. Conf. Computer Tool(EUROCON 2005),* vol. 1, pp. 374-377, 2005.
[11] T. Leloup, W. E. Kazzi, F. Schuind, N. Warzee, "A Novel Technique for Dislat Locking of Intramedullary Nail Based on Two Non-Constrained Fluoroscopic Images and Navigation," *IEEE Trans. Med. Image.,* vol. 27, pp. 1202-1212, 2008.
[12] G. Zheng, X. Zhang, L.P. Nolte, "Automatic Pose Recovery of the Distal Locking Holes from Single Calibrated Fluoroscopic Image for Computer-Assisted Intramedullary Nailing of Fermoral Shaft Fractures," *MIAR 2006,* pp. 195-202, 2006.

[13] G. Zheng, X. Zhang, D. Haschtmann, P. Gedet, X. Dong, L.P. Nolte, "A Robust and Accurate Two-Stage Approach for Automatic Recovery of Distal Locking Holes in Computer-Assisted Intramedullary Nailing of Femoral Shaft Fractures," *IEEE Trans. Med. Image.,* vol. 27, pp. 171-187, 2008.

[14] L. Joskowicz, C. Milgrom, M. Shoham, Z. Yaniv, A. Simkin, "Robot-guided long bone intramedullary distal locking concept and preliminary results," *In Proc. Computer Assisted Rodiology and Surgery,* pp. 485-491, 2003.

[15] Z. Yaniv and L. Joskowicz, "Precise robot-assisted guide positioning for distal locking of intramedullary nails," *IEEE Trans. Med. Img.,* vol. 24, pp. 624-635, 2005.

[16] Du Zhi-jiang, K. Min-xiu,Fu Li-xin, Sun Li-ning, "A Novel Fluoroscopy-Guided Robot-Assisted Orthopaedic Surgery System," *Int. conf. on Robotics and Biomimetics,* pp. 1622-1627, 2006.

[17] B. Diotte, P. Fallavollita, L. Wang, S. Weidert, E. Euler, P. Thaller, N. Navab, “Multi-modal intra-operative navigation during distal locking of intramedullary nails,” *IEEE Trans. Med. Imaging*., vol. 34, pp. 487-95, 2015.

[18] R. Londei, M. Esposito, B. Diotte, S. Weidert, E. Euler, P. Thaller, N. Navab, P. Fallavollita, “Intra-operative augmented reality in distal locking,” *Int. J. Comput. Assist. Radiol. Surg.*, vol. 10, pp. 1395–1403, 2015.

[19] Nakdhamabhorn, S., and Suthakorn, J., "A Novel Surgical Navigation Concept for Closed Intramedullary Nailing of Femur Using 4-DOF Laser-Guiding Robot," *Proceedings of the 2011 IEEE International Conference on Robotics and Biomimetics (ROBIO 2011)*, pp 479-484, 2011.

[20] Liang, J.T., Doke, T., Onogi, S., Ohashi, S., Ohnishi, I., Sakuma, I., Nakajima, Y., “A fluorolaser navigation system to guide linear surgical tool insertion,” *Int. J. Comput. Assist. Radiol. Surg.*, vol. 7(6), pp. 931–939,2012.

[21] Fitzgibbon, A. W., Pilu, M and Fischer, "Direct least squares fitting of ellipses," *Int. conf. on Pattern Recognition,* pp. 253-257, 1996.

[22] Z. Zhang, “A flexible new technique for camera calibration,” *IEEE Transactions on Pattern Analysis and Machine Intelligence* Vol. 22, Issue: 11, Nov 2000.

[23] R. Hartley and A. Zisserman, "Multiple View Geometry in Computer Vision," pp.178-181, 2003.

[24] Mohammad Reza Elhami, Iman Dashti, “A New Approach to the Solution of Robot Kinematics Based on Relative Transformation Matrices,” *International Journal of Robotics and Automation,* Vol.5, pp.213-22, 2016.

[25] Pillai, B., M., and Suthakorn, J., “Motion Control Applications: Observer Based DC Motor Parameters Estimation for Novices," *International Journal of Power Electronics and Drive Systems (IJPEDS)*, Vol. 10 (1), pp. 195-210, 2019.